

# Charge carrier induced lattice strain and stress effects on As activation in Si

Chihak Ahn<sup>1,a)</sup> and Scott T. Dunham<sup>1,2</sup>

<sup>1</sup>Department of Physics, University of Washington, Seattle, Washington 98195, USA

<sup>2</sup>Department of Electrical Engineering, University of Washington, Seattle, Washington 98195, USA

(Received 15 January 2008; accepted 18 June 2008; published online 17 July 2008)

We studied lattice expansion coefficient due to As using density functional theory with particular attention to separating the impact of electrons and ions. Based on As deactivation mechanism under equilibrium conditions, the effect of stress on As activation is predicted. We find that biaxial stress results in minimal impact on As activation, which is consistent with experimental observations by Sugii *et al.* [J. Appl. Phys. **96**, 261 (2004)] and Bennett *et al.* [J. Vac. Sci. Technol. B **26**, 391 (2008)]. © 2008 American Institute of Physics. [DOI: 10.1063/1.2956401]

Stress effects are of great interest in modern ultra-large scale integration (ULSI) technology since they can be employed to improve various material properties. Uniaxial stress has been employed in metal oxide-semiconductor field-effect transistor (MOSFET) devices since the 90 nm node technology step to improve carrier mobility.<sup>1</sup> Properly applied stress can also suppress dopant diffusion,<sup>2-4</sup> enhance activation,<sup>3,5,6</sup> and reduce the band gap.<sup>7</sup> Therefore, understanding stress effects becomes essential for further MOSFET scaling.

As deactivation is governed by  $As_mV_n$  cluster formation, and clusters with  $m=1-4$  and  $n=1$  are considered as the dominant species in deactivation kinetics.<sup>8</sup> Under equilibrium conditions, the concentrations of defect X (As, V, or  $As_mV$ ) are determined by the free As and V concentrations and cluster formation energies:  $C_X = A \exp(-E_X^f/kT)$ , where  $E_X^f$  is the formation enthalpy, and A includes the configuration and formation entropy. The total chemical As concentration is given by

$$C_{As}^{\text{total}} = C_{As} + \sum_{m=1}^4 m C_{As_mV}. \quad (1)$$

Table I lists the formation energies of  $As_mV$  complexes based on the total free energy of 64 atom (or 63 atom, with vacancy) supercells using the density functional theory (DFT) code<sup>9</sup> VASP with PW91 generalized gradient approximation (GGA) functional.<sup>10</sup> All calculations were done at a 250 eV energy cutoff with 2<sup>3</sup> Monkhorst-Pack **k**-point sampling.<sup>11</sup> Each time an As atom is added to a vacancy, the formation energy is lowered by about 1.5 eV, and thus a larger complex is more stable than a smaller one. We calculated the  $As_mV$  concentrations based on the formation energies listed in Table I. Since DFT GGA underestimates the vacancy formation energy by about 1 eV,<sup>12</sup> we also applied a correction for the  $As_mV$  formation energies using experimental values.<sup>13</sup>  $As_4V$  has the lowest formation energy and becomes the dominant cluster under equilibrium conditions. Smaller clusters can be formed during epitaxial As-doped Si growth and early stages of annealing, and can dominate before full equilibration is reached,<sup>14,15</sup> but we restrict our analysis to equilibrium conditions.

<sup>a)</sup>Electronic mail: chahn@u.washington.edu.

Figure 1 shows the isolated As concentration as a function of the total As concentration. As the number of As forming  $As_4V$  increases to become a significant fraction of free As, the free As concentration starts deviating from the total chemical As concentration, which is consistent with previous reports.<sup>15,16</sup> We should note that the  $As_4V$  formation energy is actually Fermi level dependent due to a charge transfer from the Fermi level to the cluster when  $As_4V$  forms. A higher Fermi level results in lower cluster formation energies, and thus the  $As_4V$  (As) curve becomes steeper (flatter) when the Fermi level dependent formation energy is used. Figure 1 uses  $E_F = E_c$ , which is appropriate for degenerately doped Si.

The change in the equilibrium concentration of X due to strain is given by

$$\frac{C_{As_mV}(\boldsymbol{\epsilon})}{C_{As_mV}(0)} \approx \left[ \frac{C_{As}(\boldsymbol{\epsilon})}{C_{As}(0)} \right]^m \exp \left[ - \frac{\Delta E_{As_mV}^f(\boldsymbol{\epsilon})}{kT} \right], \quad (2)$$

where  $\Delta E_{As_mV}^f$  is the formation energy of the defect cluster and it is given by<sup>17</sup>

$$\Delta E_{As_mV}^f(\boldsymbol{\epsilon}) = -V_0(\Delta \boldsymbol{\epsilon}_{As_mV} - m \Delta \boldsymbol{\epsilon}_{As}) \cdot \mathbf{C} \cdot \boldsymbol{\epsilon}, \quad (3)$$

where  $V_0$  is the volume of a lattice site,  $\Delta \boldsymbol{\epsilon}_X$  is the induced strain due to X, **C** is the elastic stiffness tensor of Si, and  $\boldsymbol{\epsilon}$  is applied strain. The induced strain can be determined from energy versus strain curves<sup>6</sup> and the results are summarized in Table II. Due to symmetry, induced strains of As, AsV, and  $As_4V$  are isotropic (hydrostatic). We repeated calculations using 216 atom supercell for selected structures and acquired the same induced strains.

TABLE I. Formation energy of  $As_mV$  clusters. When the experimental vacancy formation energy [4.60 eV (Ref. 13)] is used, formation energies increase by about 1 eV. The experimental value of the V formation energy was calculated by subtracting the migration barrier (0.26 eV, DFT value) from the activation enthalpy [4.86 eV (Ref. 13)]. In the second row, the first value is based on the DFT result, and the second is based on the experimental V formation energy.

	V	AsV	As <sub>2</sub> V	As <sub>3</sub> V	As <sub>4</sub> V
$E^f$ (eV)	3.59	2.15	0.68	-0.66	-2.22
	4.60	3.16	1.69	0.35	-1.21

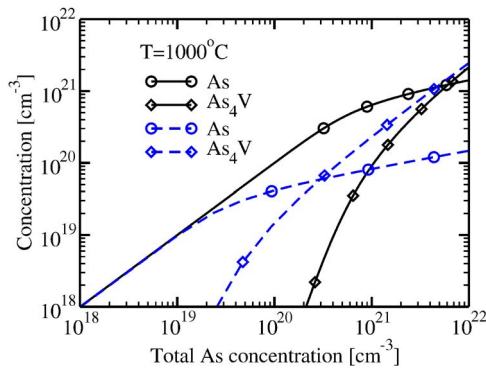


FIG. 1. (Color online) Equilibrium As concentration and  $As_4V$  concentration as a function of the total chemical As concentration for  $E_F = E_c$ . Solid lines are plotted with correction for vacancy formation energy and broken lines are plotted with DFT formation energies. Smaller clusters don't appear due to low concentration.

TABLE II. Induced hydrostatic strain [ $\Delta\bar{\epsilon} = (\Delta\epsilon, \Delta\epsilon, \Delta\epsilon)$ ] for As and  $As_mV$  complexes. As produces small lattice expansion and  $As_mV$  complexes result in lattice contraction.

	As	V	AsV	As <sub>2</sub> V	As <sub>3</sub> V	As <sub>4</sub> V
$\Delta\epsilon$	0.018	-0.25	-0.21	-0.22	-0.11	-0.08

TABLE III. Induced hydrostatic strain due to As,  $As^+$ , and free electrons and holes. The numbers in parentheses are extracted from Cargill *et al.* (Ref. 18). Note that in spite of longer As–Si bond length in  $Si_{63}As^+$  supercell (Table IV), the lattice undergoes contraction.

	As <sup>0</sup>	As <sup>+</sup>	e <sup>-</sup>	h <sup>+</sup>
$\Delta\epsilon$	0.018 (-0.019)	-0.22 (0.07)	0.22 (-0.09)	-0.26

TABLE IV. Local lattice structure around an As atom in the Si lattice compared to atomic spacing in pure Si.

	Si	As <sup>0</sup>	As <sup>+</sup>	As (exp) <sup>a</sup>
1NN	2.36	2.45	2.43	2.43
2NN	3.86	3.87	3.86	3.87
3NN	4.53	4.53	4.52	4.53

<sup>a</sup>Reference 19.

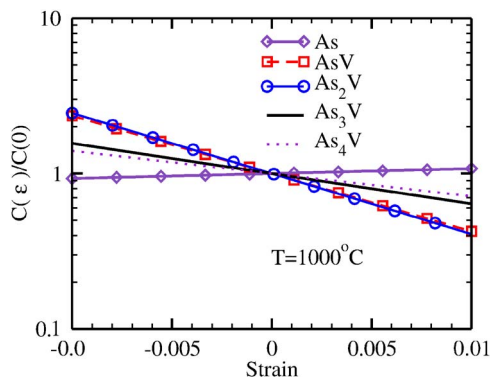


FIG. 2. (Color online) Stress effects on As and  $As_mV$  cluster concentration under biaxial stress. Note that the two dominant complexes, As and  $As_4V$ , have minimal stress effects.

As shown in Table II, DFT predicts a small lattice expansion due to As. However, several authors have observed lattice contractions in heavily As-doped Si, which they attributed to free electrons in the conduction band.<sup>18–20</sup> In contrast to their conclusion, DFT calculations predict a lattice expansion due to free electrons in the conduction band (Table III). In the work of Cargill *et al.*, the total induced strain ( $\Delta\epsilon_{As} = \beta_{total}N_{As}$ ) is assumed to be given by the sum of the induced strain due to ions ( $\Delta\epsilon_{As^+} = \beta_{size}N_{As}$ ) and free electrons ( $\Delta\epsilon_e = \beta_eN_{As}$ ). As shown in Table III, the calculated induced strain due to  $As^0$  has opposite sign to measured value, but the absolute difference is small and thus its impact on stress effects is minimal. However, the reasoning is very different in each case, which raises a fundamental question about the role of electrons. Do electrons cause expansion or contraction in the lattice? To answer this question, we performed DFT calculations to find equilibrium lattice constants of charged and neutral supercells with various group III and IV elements and concluded that electrons expand the lattice while holes cause lattice contraction.

The lattice expansion due to electrons raises another question about the relation between Si–As bond length and the lattice parameter. We looked into the local structure around As in Si matrix to answer this question. As listed in Table IV, DFT calculations agree with experimental measurement up to the third nearest neighbor (3NN) distance and predict a local volume expansion around As.<sup>16,21,22</sup> However, this expansion is attenuated as distance increases and As–Si 3NN spacing is very similar to Si–Si 3NN distance. Therefore, changes in the first nearest neighbor (1NN) bond length are not directly linked to changes in the lattice parameter, and care should be taken when linking short range atomic spacing to lattice constant. In fact,  $As^+$  produces a lattice contraction ( $\Delta\epsilon = -0.22$ ) in spite of longer As–Si bond length. A free electron in the conduction/impurity band overcompensates this contraction, and thus neutral As results in an overall tiny expansion ( $\Delta\epsilon = 0.018$ ).

Based on our analysis, it is likely that experimentally observed lattice contractions originate from reasons other than free electrons. We attribute them to high concentrations of vacancies in the form of  $As_mV_n$  clusters, and find that a vacancy concentration of about 15% of the As concentration can reproduce the lattice contraction observed by Cargill *et al.*<sup>18</sup> This level of vacancy concentration was reported based on *ab initio* calculations by Berding *et al.*<sup>8</sup> and positron annihilation spectroscopy by Borot *et al.*<sup>23</sup>

Effects of stress on As and  $As_mV$  concentrations are plotted in Fig. 2 based on Eq. (2). The concentrations of the two dominant configurations, As and  $As_4V$ , undergo changes in opposite directions under biaxial stress, but the magnitude is minimal due to the small induced strain. Finally, the free As concentration as a function of the total As concentration is plotted in Fig. 3. At a given total As concentration, compressive biaxial stress enhances  $As_mV$  formation, and thus the number of active As decreases. However, stress effects are minimal due to the small induced strains of dominant structures, in accordance with previous experiments.<sup>24,25</sup>

In conclusion, by performing DFT calculations of the local structure around As in the silicon lattice, we found that lattice expansion due to the larger size of an As atom is limited to within 3NN distances. The lattice contraction in highly As-doped Si can be explained by  $As_mV$  cluster formation rather than free electron as previously suggested.<sup>18</sup> The

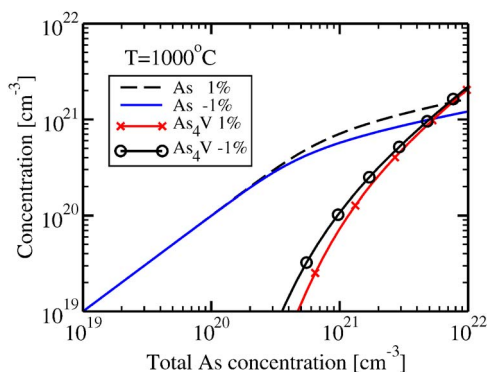


FIG. 3. (Color online) Equilibrium concentrations of As and  $As_mV$  cluster as a function of total As concentration under biaxial stress.

small induced strain due to both isolated As and the dominant deactivated cluster  $As_4V$  results in negligible stress effects on the carrier concentration, in accordance with experimental observations.<sup>24,25</sup>

This research was supported by the Semiconductor Research Corporation (SRC). Computer hardware used in this work was provided by donations from Intel and AMD as well as NSF Award No. EIA-0101254.

<sup>1</sup>S. E. Thompson, M. Armstrong, C. Auth, M. Alavi, M. Buehler, R. Chau, S. Cea, T. Ghani, G. Glass, T. Hoffman, C.-H. Jan, C. Kenyon, J. Klaus, K. Kuhn, Z. Ma, B. McIntyre, K. Mistry, A. Murthy, B. Obradovic, R. Nagisetty, P. Nguyen, S. Sivakumar, R. Shaheed, L. Shifren, B. Tufts, S. Tyagi, M. Bohr, and Y. El-Mansy, *IEEE Trans. Electron Devices* **51**, 1790 (2004).

<sup>2</sup>N. Moriya, L. C. Feldman, H. S. Luftman, C. A. King, J. Bevk, and B. Freer, *Phys. Rev. Lett.* **71**, 883 (1993).

<sup>3</sup>T. T. Fang, W. T. C. Fang, P. B. Griffin, and J. D. Plummer, *Appl. Phys. Lett.* **68**, 791 (1996).

<sup>4</sup>C. Ahn, J. Song, and S. T. Dunham, *Semiconductor Defect Engineering—Materials, Synthetic Structures and Devices II*, MRS Symposia Proceedings No. 913 (Materials Research Society, Pittsburgh, 2006), Vol. 994, p. 275–279.

<sup>5</sup>R. F. Lever, J. M. Bonar, and A. F. W. Willoughby, *J. Appl. Phys.* **83**,

1988 (1998).

<sup>6</sup>C. Ahn and S. T. Dunham, *J. Vac. Sci. Technol. B* **24**, 700 (2006).

<sup>7</sup>L. Yang, J. R. Watling, R. C. W. Wilkins, M. Borici, J. R. Barker, A. Asenov, and S. Roy, *Semicond. Sci. Technol.* **19**, 1174 (2004).

<sup>8</sup>M. A. Berding, A. Sher, M van Schilfgaard, P. M. Rousseau, and W. E. Spicer, *Appl. Phys. Lett.* **72**, 1492 (1998).

<sup>9</sup>G. Kresse and J. Hafner, *Phys. Rev. B* **47**, RC558 (1993); G. Kresse and J. Furthmüller, *ibid.* **54**, 11169 (1996).

<sup>10</sup>J. P. Perdew, J. A. Chevary, S. H. Vosko, K. A. Jackson, M. R. Pederson, D. J. Singh, and C. Fiolhais, *Phys. Rev. B* **46**, 6671 (1992).

<sup>11</sup>A. Baldereschi, *Phys. Rev. B* **7**, 5212 (1973); D. J. Chadi and M. L. Cohen, *ibid.* **8**, 5747 (1973); H. J. Monkhorst and J. D. Pack, *ibid.* **13**, 5188 (1976).

<sup>12</sup>E. R. Batista, J. Heyd, R. G. Henning, B. P. Uberuaga, R. L. Martin, G. E. Scuseria, C. J. Umrigar, and J. W. Wilkins, *Phys. Rev. B* **74**, 121102 (2006).

<sup>13</sup>A. Ural, P. B. Griffin, and J. D. Plummer, *Phys. Rev. Lett.* **83**, 3454 (1999).

<sup>14</sup>V. Ranki, J. Nissilä, and K. Saarinen, *Phys. Rev. Lett.* **88**, 105506 (2002).

<sup>15</sup>M. Derdour, D. Nobili, and S. Solmi, *J. Electrochem. Soc.* **138**, 857 (1991).

<sup>16</sup>A. Erbil, W. Weber, G. S. Cargill, and R. F. Boehme, *Phys. Rev. B* **34**, 1392 (1986).

<sup>17</sup>M. Diebel, S. Chakravarthi, S. T. Dunham, and C. F. Machala, Simulation of Semiconductor Processes and Devices—SISPAD 2004 (unpublished), p. 37.

<sup>18</sup>G. S. Cargill III, J. Angilello, and K. L. Kavanagh, *Phys. Rev. Lett.* **61**, 1748 (1988).

<sup>19</sup>A. Parisini, A. Bourret, A. Armigliato, M. Servidori, S. Solmi, R. Fabbri, J. R. Regnard, and J. L. Allain, *J. Appl. Phys.* **87**, 2320 (1990).

<sup>20</sup>A. Herrera-Gomez, P. M. Rousseau, T. Kendelewicz, J. C. Woicik, J. Plummer, and W. E. Spicer, *J. Appl. Phys.* **85**, 1429 (1999).

<sup>21</sup>V. Koteski, N. Ivanovic, H. Haas, E. Holub-Krappe, and H.-E. Mahnke, *Nucl. Instrum. Methods Phys. Res. B* **200**, 60 (2003).

<sup>22</sup>S. Wei, H. Oyanagi, H. Kawanami, K. Sakamoto, T. Sakamoto, K. Tamura, N. L. Saini, and K. Uosaki, *J. Appl. Phys.* **82**, 4810 (1997).

<sup>23</sup>G. Borot, L. Rubaldo, L. Clement, R. Pantel, D. Dutartre, K. Kuitunen, J. Slotte, F. Tuomisto, X. Mescot, M. Gri, and G. Ghibaudo, *J. Appl. Phys.* **102**, 103505 (2007).

<sup>24</sup>N. Sugii, S. Irieda, J. Morioka, and T. Inada, *J. Appl. Phys.* **96**, 261 (2004).

<sup>25</sup>N. Bennett, A. J. Smith, R. M. Gwilliam, R. P. Webb, B. J. Sealy, N. E. B. Cowern, L. O'Reilly, and P. J. McNally, *J. Vac. Sci. Technol. B* **26**, 391 (2008).